





# Naturally Occurring Quorum Sensing Inhibitors for *Pseudomonas aeruginosa* by Molecular Modeling

Mohammad Mohajeri <sup>1</sup>, Samad Nejad Ebrahimi <sup>1,\*</sup>, Mohamadreza Gholamnia <sup>1</sup>, Mohammad Bayati <sup>1</sup>

<sup>1</sup> Department of Phytochemistry, Medicinal Plants and Drugs Research Institute, Shahid Beheshti University, Tehran, Iran

\* Correspondence: [s\\_ebrahimi@sbu.ac.ir](mailto:s_ebrahimi@sbu.ac.ir) (S.N.E.);

Scopus Author ID 9338406700

Received: 2.01.2022; Accepted: 10.02.2022; Published: 27.03.2022

**Abstract:** The quorum-sensing (QS) system allows organisms to communicate and form virulence factors such as biofilm. *Pseudomonas aeruginosa* is one of the Gram-negative bacteria leaving many casualties every year. In the past years, the bacteria's QS system has gained attention as a valuable target to design and develop new efficient antibiotics. Nature has always been an inspiration source for designing many new medicines, and using natural compounds is always the first approach to discover and design new drugs. Here, we *in-silico* studied 24,000 natural compounds, including first and secondary metabolites, on five known QS-related receptors of *Pseudomonas aeruginosa*. After several levels of screening, compounds NP-1 (3,6'-di-O-sinapoylsucrose), NP-2 (ZINC000257412737), NP-3 (3-O-β-D-rutinosin) showed the best inhibition activity on AHL synthase LasI with the docking scores of -8.988, -8.690, and -8.925 kcal/mol, respectively. Also, NP-101 (ZINC000077264779), NP-102 (ZINC000225518732), and NP-103 (ZINC000096269362) were selected for LasR-LBD with the scores of -13.355, -13.038, and -12.917 kcal/mol, respectively. In the case of LasA, docking scores of -13.357, -10.796, and -10.564 kcal/mol were obtained for NP-201 (Parishin), NP-202 (7-O-galloyl-D-sedoheptulose), and NP-203 (1,2-di-O-galloyl-6-O-p-coumaroyl-β-D-glucose), respectively. Furthermore, when the LasR-TP4 was the target, the best results were observed from NP-301 (ZINC000514288841), NP-302 (ZINC000077264754), and again NP-103 (ZINC000096269362), in which they showed docking scores of -13.175, -13.020, and -12.998 kcal/mol, respectively. Finally, the highest docking scores belonged to NP-401 (ZINC000150351649), NP-402 (ZINC000150351636), NP-403 (ZINC000150349056), which interacted with the ATPase Type IV pilus with the docking scores of -16.274, -15.773, and -15.405 kcal/mol, respectively.

**Keywords:** antibacterial; molecular modeling; natural products; *Pseudomonas aeruginosa*; quorum sensing inhibition.

© 2022 by the authors. This article is an open-access article distributed under the terms and conditions of the Creative Commons Attribution (CC BY) license (<https://creativecommons.org/licenses/by/4.0/>).

## 1. Introduction

*Pseudomonas aeruginosa* is the most common Gram-negative bacteria involving about 11% of nosocomial infections worldwide. Due to its numerous virulence factors that can break through the human's defense system and cause different topical and systemic diseases [1-3]. Biofilm formation is one of the virulence factors which plays an essential role in protecting *P. aeruginosa* against the host defense mechanisms and antibiotics [4, 5]. The cell to cell signaling communication mechanism in the biofilm colonies, which controls the cell functions, is defined as Quorum Sensing (QS) system [3, 6]. QS is how a single bacterium produces small diffusible molecules detected by neighboring organisms. Acyl-homoserine lactone (AHL) is one of the

signaling molecules in most Gram-negative bacteria such as *P. aeruginosa*. This communication mechanism enables bacteria to act as a community in the coordinated regulation of gene expression. This regulated expression of virulence genes is vital for the organism's pathogenesis [7].

There are two QS systems in *P. aeruginosa*, including the Las and Rhl systems [8]. The Las system consists of the LasR transcriptional regulator and the LasI synthase protein [9]. As has been reported previously, LasI is essential for the production of the AHL signal molecule *N*-(3-oxododecanoyl)-L-homoserine lactone (3-oxo-C12-HSL) [10, 11]. The existence of 3-oxo-C12-HSL in the environment causes LasR to form multimers, and subsequently, the multimeric form of the LasR binds DNA and regulates the transcription of multiple genes [12]. On the other hand, two vital proteins such as RhlI and RhlR involve in the Rhl system. The RhlI synthase generates the AHL *N*-butyryl-L-homoserine lactone (C4-HSL) in this signaling system. The complex formation of C4-HSL with the RhlR leads to the expression of several genes by RhlR [13, 14]. In conclusion, quorum sensing inhibition in *P. aeruginosa* can be achieved by targeting different proteins and pathways in the Las and Rhl system [7].

Natural products always have been a promising drug source for many purposes [15, 16]. In particular, some of them show significant anti-QS activity due to the co-existence of plants and fungi with bacteria for million years. This long co-existence between yeasts, plants, and bacteria resulted in the development and evolution of their defensive mechanisms against different pathogens by applying various strategies such as disrupting the molecular communication of bacteria [17, 18]. In Table 1, selected previously reported medicinal and dietary plants that have exhibited QS inhibitory activity are shown. For instance, in 2017, a study revealed that *Terminalia bellerica*'s leaves could significantly inhibit violacein production in *C. violaceum* and reduce biofilm formation in *P. aeruginosa* [19]. In another study, it was observed that the fruit of *Vaccinium Macrocarpon* shows anti-virulence activity against elastase (LasA and LasB) in both *P. aeruginosa* and *C. violaceum* [20, 21]. Furthermore, *Andrographis Paniculata* has been reported to have inhibition effects on protease, elastase, pyocyanin, swimming motility, and biofilm in *C. violaceum* and *P. aeruginosa* [22]. Also, *Artemisia argyi* leaf extracts have exposed QS inhibition toward PAO1 [23].

The selected target receptors to interfering quorum-sensing system in *P. aeruginosa* were included: I) AHL synthase LasI (PDB ID: 1RO5) [24], II) LasR-LBD (PDB ID: 2UV0) [25], III) LasA (PDB ID: 3IT7) [26], IV) LasR-TP4 (PDB ID: 3JPU) [27], and V) ATPase Type IV pilus (PDB ID: 3JVV) [28]. These receptors were selected based on their QS role in *P. aeruginosa*. AHL synthase LasI is responsible for the Secretion of 3-oxo-C12-HSL from 3-oxo-C12-acyl carrier protein (acyl-ACP) and S-adenosyl-L-methionine [24]. The accumulation of 3-oxo-C12-HSL with population growth in the bacteria activates LasR, a transcriptional regulator homologous to LuxR. LasR activation leads to the binding of LasR dimers to target gene promoters and subsequently activates the transcription of several toxic virulence factors such as exotoxins, exoproteases, and secondary metabolites. Besides, activated LasR takes part in the maturation of biofilms, which usually eventuate in persistent pathogenic infection [25]. In addition to LasI and LasR, LasA is also involved in several processes related to *P. aeruginosa* virulence, namely elastin degradation in connective tissue [26, 29]. Thus, it is a valuable target to attenuate the pathogenicity of *P. aeruginosa*. Finally, the last target receptor was ATPase Type IV pilus. Type IV pili (TFp) are extracellular appendages that exist in many bacteria. Although they are not vital for viability, they play an essential role in the lifecycle of many bacteria by participating in cell adhesion, phage and DNA uptake, twitching motility,

and biofilm formation [28]. Hence, disrupting the mechanisms that power pilus assembly and disassembly can significantly debilitate the bacteria to use pili for virulence.

In this study, the virtual screening of the 24,000 compounds against the five targets was carried out using high throughput virtual screening (HTVS). The top 100 structures for each receptor entered the next phase and were evaluated by the extra precision (XP) docking method. Binding free energies, as well as pharmacokinetic characteristics (ADMET), were calculated for hit candidates. Finally, the top three promising *in silico* inhibitors for each of the five QS receptors in *P. aeruginosa* were identified and reported.

**Table 1.** The anti-QS activity of some medicinal and dietary plants.

Plant name	Part used	Biosensorstrain(s)	Virulence factor(s) inhibited	References
<i>Pelargonium hortorum</i>	Aerial parts	<i>P. aeruginosa</i>	Motility	[30]
<i>Punica granatum</i>			Pyocyanin	
<i>Artemisia absinthium</i>			LasA protease	
<i>Hibiscus sabdariffa</i>				
<i>Momordica charantia</i>				
<i>Forsythia suspense</i>	Aerial parts	<i>C. violaceum</i> ATCC 12472	Pyocyanin, protease, biofilm, and motility	[31]
		<i>P. aeruginosa</i>		
<i>Amomum tsaoko</i>	Fruit pods	<i>C. violaceum</i>	Pyocyanin, biofilm, and motility	[32]
		<i>P. aeruginosa</i>		
<i>Terminalia bellerica</i>	Leaves	<i>C. violaceum</i> ATCC 12472	EPS, pyocyanin, and biofilm	[19]
		<i>P. aeruginosa</i> PA01		
<i>Vaccinium macrocarpon</i>	Fruit	<i>P. aeruginosa</i> PA14 QS Mutants	Elastase (LasA and LasB), alkaline protease	[20]
<i>Vaccinium macrocarpon</i>	Fruit	<i>C. violaceum</i> ATCC 31532	Elastase (LasA and LasB), alkaline protease	[20]
<i>Cassia alata</i>	Leaves	<i>C. violaceum</i> ATCC 12472	Swarming motility, pyocyanin, LasB, elastase, protease, and biofilm	[33]
		<i>C. violaceum</i> CV026		
		<i>C. violaceum</i> ATCC 31532		
		<i>P. aeruginosa</i> PAO1		
<i>Trigonella foenum-graceum</i>	Seed	<i>C. violaceum</i> ATCC 12472	Elastase, protease, pyocyanin, EPS, chitinase, swarming, and biofilm	[34, 35]
		<i>C. violaceum</i> CV026		
		<i>P. aeruginosa</i> PAO1		
<i>Psidium guajava</i>	Leaves	<i>C. violaceum</i> MTCC 2656	Violence and swarming motility	[36]
		<i>P. aeruginosa</i> MTCC 2297		
<i>Dalbergia trichocarpa</i>	Bark	<i>P. aeruginosa</i> PAO1 QS mutants	Pyocyanin, LasB, protease, biofilm, and swarming motility	[37]
<i>Fructus gardenia</i>	Whole plant	<i>C. violaceum</i> ATCC 12472	Protease, elastase, pyocyanin, swimming, motility, and biofilm	[22]
<i>Andrographis paniculata</i>		<i>P. aeruginosa</i> PAO1		

## 2. Materials and Methods

### 2.1. 3D-ligand preparation & protein preparation.

The structures of 24,000 bioactive natural compounds were obtained from the ZINC15 database (<https://zinc15.docking.org/>). The entire compounds were optimized using the OPLS3 force field, and by applying Epik in the pH range of  $7.0 \pm 2$ , conformations were generated. The compounds were desalted and tautomerized. Sixteen stereoisomers and four low energy ring conformation were made per ligand for computation using the Ligprep module of Maestro.

The crystallography structures of the five target receptor including AHL synthase LasI (PDB ID: 1RO5), LasR-LBD (PDB ID: 2UV0), LasA (PDB ID: 3IT7), LasR-TP4 (PDB ID: 3JPU), and ATPase Type IV pilus (PDB ID: 3JVV) were downloaded from the Protein Data Bank (<https://www.rcsb.org/>). Proteins were prepared using the Protein Preparation Wizard Tool of Maestro (2015). To this end, hydrogen atoms were added to the receptors, disulfide and zero-order metal bonds were created in the protein's chains. The water molecules that do not participate in interactions, the native ligand, and the heteroatom(s) were removed. The PROPKA was employed to predict the pKa of ionizable groups in proteins at pH 7.00. Ultimately, the OPLS3 force field was optimized and minimized at RMSD of 0.3 Å the proteins.

## 2.2. Identification of the active sites & receptor grid box generation.

The active site of each receptor was determined by identifying the amino acids bound to the native ligand. Also, the amino acids involved in the complex formation and, consequently, the active site of each protein was obtained as follows:

**I)** AHL synthase LasI: Arg30, Met125, Ala155, Thr144, Arg130, Val148, Lys150, Arg154, Ser103, Glu101

**II)** LasR-LBD: Thr75, Val76, Trp60, Tyr69, Cys79, Ala105, Tyr93, Leu110, Gly126, Ser129

**III)** LasA: His23, Asp36, Tyr80, His81, Ser115, Ala118, His188, Gly286, Gly309, Thr304

**IV)** LasR-TP4: Ala50, Tyr47, ILE52, Trp88, Phe101, Leu110, Gly126, Asp173, Cys179

**V)** ATPase Type IV pilus: HID229, Thr132, Ser134, Pro131, Ser137, Leu109, Ala278, Arg276, MG401

Grid box generation for each receptor was performed using Maestro's Glide program, the Receptor Grid Generation section. For this purpose, the previously mentioned amino acids for predicting each receptor's active site were entered in the 'Residues Number section'. The "Dock ligand length" option was selected and adjusted on 20 Å, and the other settings have remained unchanged. Ultimately, the cubic box with the dimension (Å) of 10 × 10 × 10 for every receptor was generated.

## 2.3. Molecular docking & docking validation.

The 24,000 natural compounds were docked into the previously mentioned receptors active site using Glide high-throughput virtual screening (HTVS) followed by extra precision (XP) for the top 100 structures obtained in the HTVS method for each receptor. For optimizing the docking setting, the Ligand sampling option was set on Flexible, and the "Sample nitrogen inversion" and "Sample ring conformation" were checked, and Epik state penalties were added to the docking score. In the end, RMSD to input ligand geometries was computed. Obtain a more detailed assessment of the *in silico* activity of the three candidates for each target, and their *in-silico* results were compared with those of the positive controls: Tobramycin (Figure 1a), a well-known antibiotic that is especially effective against species of *Pseudomonas*, N-(3-Oxododecanoyl)-L-homoserine lactone (3-oxo-C12-HSL) (Figure 1b), a reported quorum-sensing signaling molecule [25], and the specified native co-crystallized ligands where existed (Figure 1c, 1d).

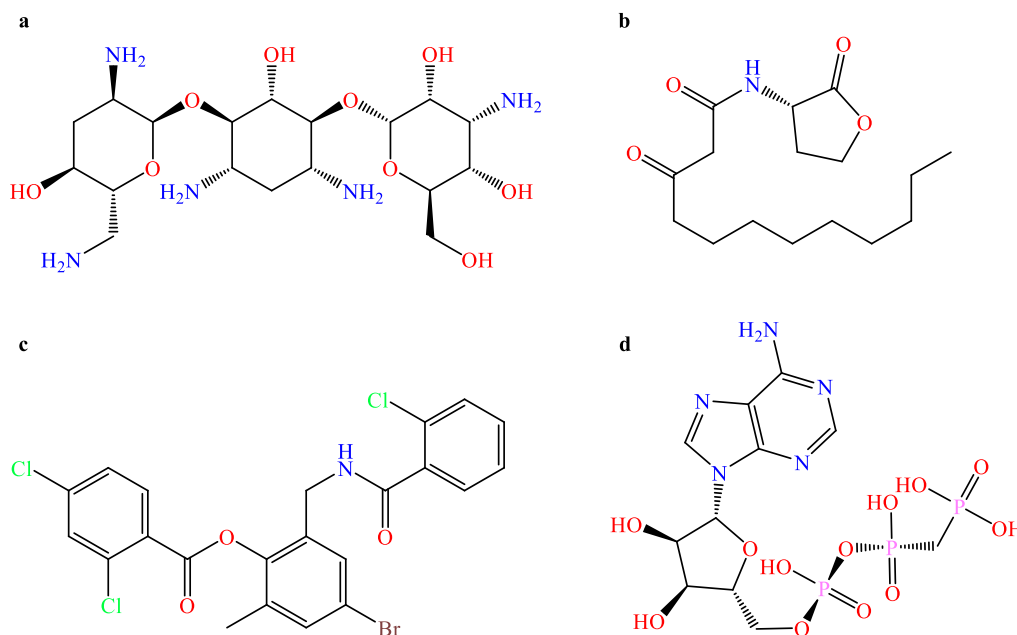


**Figure 1.** The positive controls, (a) Tobramycin; (b) N-(3-Oxododecanoyl)-L-homoserine lactone (3-oxo-C12-HSL); (c) 4-bromo-2-((2-chlorobenzamido)methyl)-6-methylphenyl 2,4-dichlorobenzoate (the native co-crystallized ligand with LasR-TP4 complex); (d) Phosphomethylphosphonic Acid Adenylate Ester (the native co-crystallized ligand with ATPase Type IV pilus).

#### 2.4. Calculating of $\Delta G_{\text{Binding}}$ .

For calculating the Gipps Free Energy of bindings, the molecular mechanics–generalized Born surface area (MM-GBSA) tool in the Prime program was used. The docking results were imported into the program, and the “Solvation model” option was set on ‘VSGB’ mode, and the calculation was performed using the OPLS3 force field. Free binding energy results were expressed in kcal/mol [38].

$$\Delta G_{\text{bind}} = G_{\text{complex}} - G_{\text{ligand}} - G_{\text{receptor}}$$

#### 2.5. Absorption, distribution, metabolism, excretion, and toxicity (ADMET) prediction.

Lipinski’s rule of five for the top 100 structures was calculated using Qikprop v4.4, updated by February 10, 2014, tool of Maestro. Pharmacokinetic aspects, namely molecular weight (MW), logPo/w, H-bond acceptor and donor, central nervous system (CNS), percentage of oral absorption, and polar surface area (PSA) were estimated for the top hit compounds.

### 3. Results and Discussion

The virtual screening protocol was applied to discover new inhibitors against different enzymes involved in the quorum-sensing process of *P. aeruginosa* (PAO1). To this end, 24,000 natural compounds, including primary and secondary metabolites, were virtually screened against five known QS-involved receptors in *P. aeruginosa* (PAO1). The target receptors were chosen carefully based on their significant roles in PAO1’s QS. At first, the entire 24,000 compounds were screened against each receptor using high throughput virtual screening (HTVS). Then, the top 100 metabolites for each protein structure were again examined by the extra precision (XP) method followed by MM-GBSA and Pharmacokinetic features calculation. The most promising three *in-silico* inhibitors for each of the targets in PAO1 were

identified and presented. The obtained data of docking and free binding energy are reported in Table 2, and the 2D structure of these hit compounds is illustrated in Figure 2.

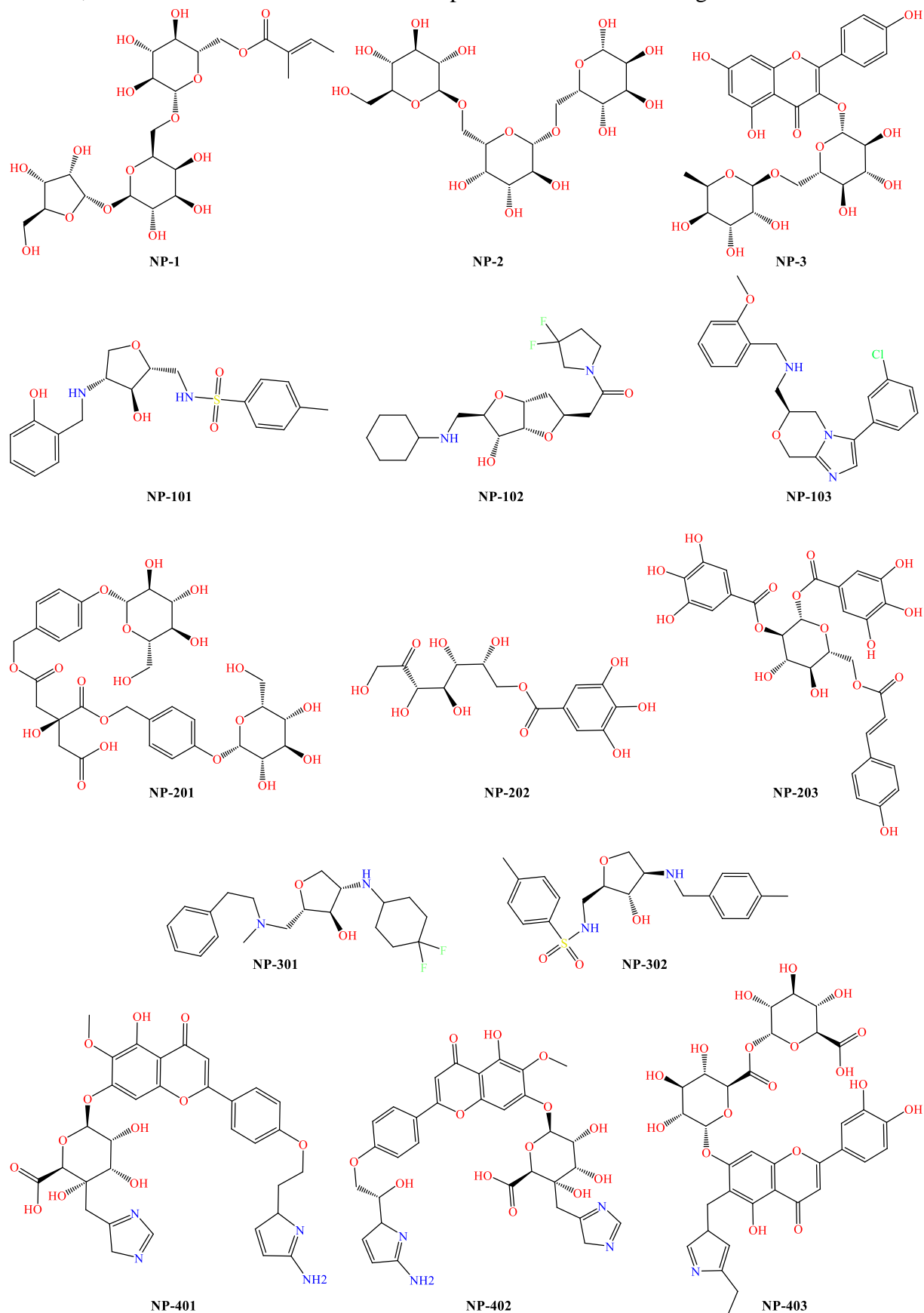


**Figure 2.** The 2D structure of hit compounds.



**Table 2.** Docking data of the top three in-silico inhibitors for each target protein.

No.	Receptor	Compound	docking score	$\Delta G_{\text{bind}}$
NP-1	AHL synthase LasI	3,6'-di-O-sinapoylsucrose	-8.988	-25.016
NP-2	AHL synthase LasI	ZINC000257412737	-8.960	-11.489
NP-3	AHL synthase LasI	3-O- $\beta$ -D-rutinosin	-8.925	-39.614
NP-101	LasR-LBD	ZINC000077264779	-13.355	-51.516
NP-102	LasR-LBD	ZINC000225518732	-13.038	-62.683
NP-103	LasR-LBD	ZINC000096269362	-12.917	-79.256
NP-201	LasA	Parishin	-13.357	-35.891
NP-202	LasA	7-O-galloyl-D-sedoheptulose	-10.796	-38.486
NP-203	LasA	1,2-di-O-galloyl-6-O-p-coumaroyl- $\beta$ -D-glucose	-10.564	-59.458
NP-301	LasR-TP4	ZINC000514288841	-13.175	-87.824
NP-302	LasR-TP4	ZINC000077264754	-13.020	-67.013
NP-103	LasR-TP4	ZINC000096269362	-12.998	-94.147
NP-401	ATPase Type IV pilus	ZINC000150351649	-16.274	-89.132
NP-402	ATPase Type IV pilus	ZINC000150351636	-15.773	-79.910
NP-403	ATPase Type IV pilus	ZINC000150349056	-15.405	-70.113

### 3.1. QS-involved receptors in PAOI.

#### 3.1.1. AHL synthase LasI.

As it is represented in Figure 3a, all three compounds showed a high docking score in comparison with the positive controls. The first compound (NP-1), 3,6'-di-O-sinapoylsucrose, has been previously reported for its anticancer properties and is extracted from *Polygala Flavescentes DC*, a sub-specie of *Polygala* family plants [39]. Hydroxyl groups in the furanose ring interact with amino acid Ile107. Also, the hydroxyl group in the pyranose ring forms hydrogen bonds with Thr145 and Glu171 (Figure 4). Amino acid Arg154 also establishes a hydrogen bond with the carboxyl group. The NP-1 with a docking score of -8.988 kcal/mol showed the most effective inhibition against AHL synthase LasI. The free binding energy for this compound was reported to be -25.016 kcal/mol. The other structure (NP-3), 3-O- $\beta$ -D-rutinosin, is the well-known main compound of *Alhagi sparsifolia* and *A. pseudalhagi*. It has been reported to have some anti-neuroinflammatory activities [40].

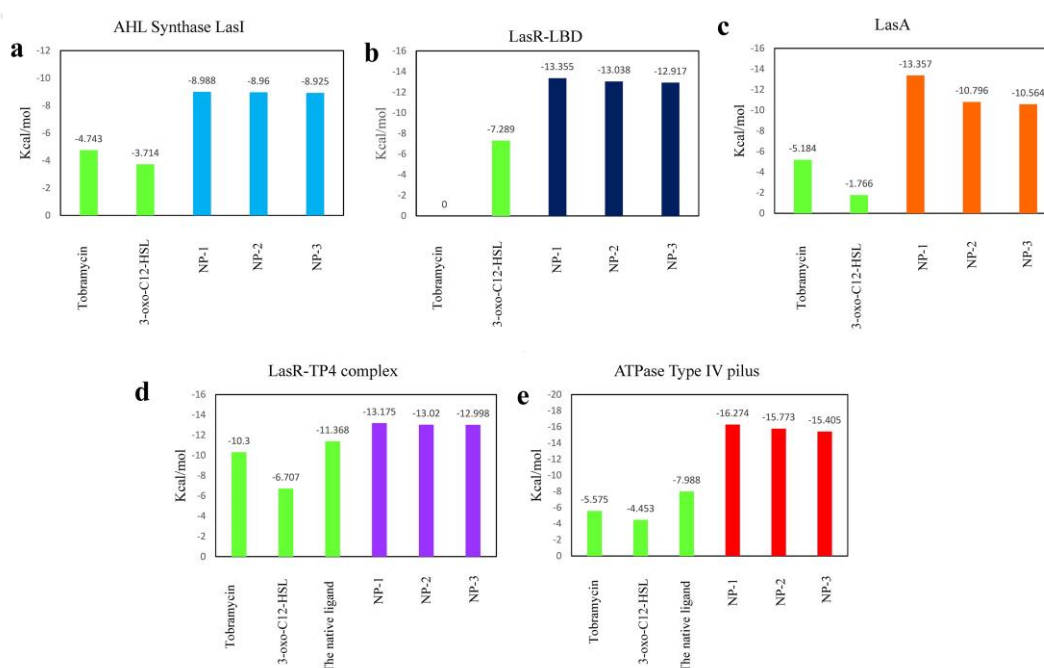


**Figure 3.** Comparison of the positive controls with the hit compounds for each receptor: (a) AHL Synthase LasI; (b) LasR-LBD; (c) LasA; (d) LasR-TP4; (e) ATPase Type IV pilus.

### 3.1.2. LasR-LBD.

According to our search, there were no previous biological activity reports related to the top three structures for this target. The native co-crystallized ligand in this protein is the same as one of the positive controls, 3-oxo-C12-HSL. This ligand showed a docking score of -7.289 kcal/mol in the interaction with its native receptor (Figure 5). In contrast, the other positive control, Tobramycin, did not show any affinity and interaction with the receptor. Meanwhile, the NP-101, NP-102, and NP-103 revealed a high attraction to LasR-LBD (Figure 3b). The compound of NP-101 with a docking score of -13.355 kcal/mol and  $\Delta G_{\text{bind}}$  of -51.516 kcal/mol was recognized as the best structure in inhibiting LasR-LBD protein. The benzene ring of the benzenesulfonamide group makes a  $\pi$ - $\pi$  stacking bond with Tyr47. The hydroxyl group of the phenolic ring forms a hydrogen bond with Trp60, and the secondary amine gives hydrogen and salt bridge bonds with Asp73.

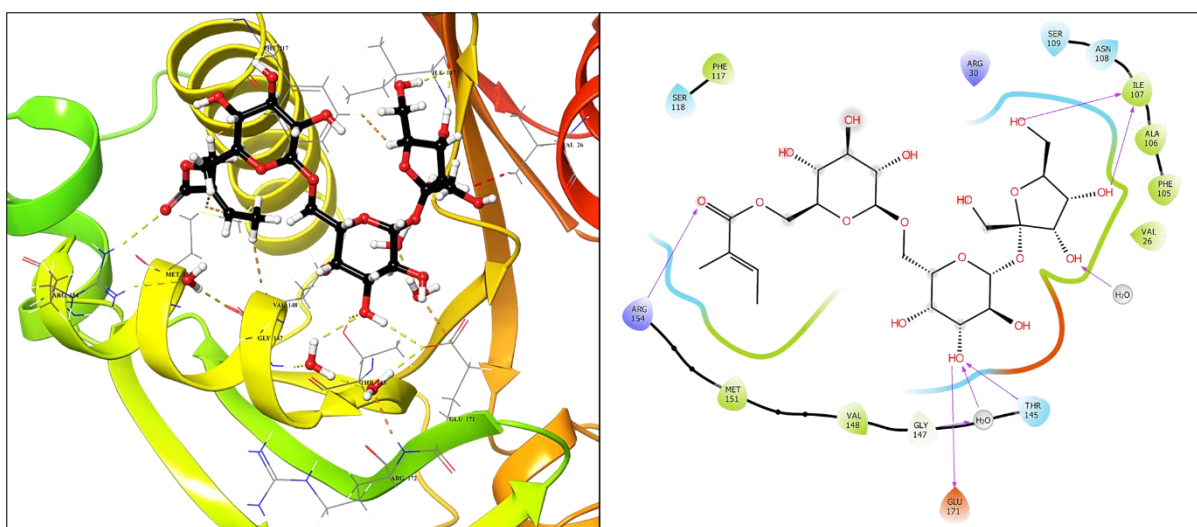


**Figure 4.** The 2D and 3D interaction of the AHL synthase LasI - 3,6'-di-O-sinapoylsucrose complex. The 2D map shows the importance of the involved amino acid in the active site.

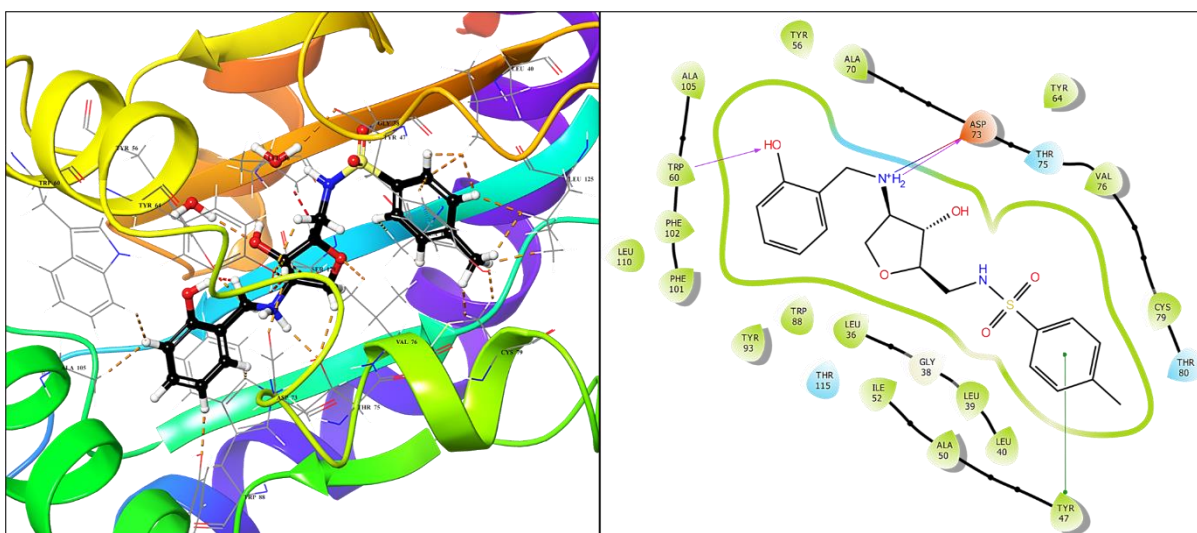


**Figure 5.** The 2D and 3D interaction of the LasR-LBD - ZINC000077264779 complex. The 2D map shows the importance of the involved amino acid in the active site.



### 3.1.3. LasA.

The first member of this group is NP-201, one of the Parish family and is extractable from rhizomes of *Gastrodia elata*. They have a history of headache, dizziness, vertigo, and convulsions epilepsy therapy [41]. Hydroxyl groups in pyranose sugar form hydrogen interactions with Gln18, Asp40, Trp41, His81, Thr117, and Tyr151. Also, Tyr151 creates a  $\pi$ - $\pi$  stacking bond with the benzene ring (Figure 6). These interactions lead to a docking score of -13.357 kcal/mol and binding free energy of -35.891 kcal/mol. The other structure with a docking score of -10.796 kcal/mol is 7-O-galloyl-D-sedoheptulose (NP-202), and it is one of the principal compounds of *Corni Fructus* and *Cornus officinalis*. It has shown some promising biological activity against Alzheimer's, diabetes, and diabetic complications. Besides, it has received attention as a preventive agent against oxidative stress-related diseases [42-50]. The last structure of the group, 1,2-di-O-galloyl-6-O-p-coumaroyl- $\beta$ -D-glucose (NP-203) with the binding energy of -59.458 kcal/mol and docking score of -10.564 kcal/mol, is one of the main constituents of Rhubarb, an important crude drug in Asiatic regions which is produced from different *Rheum* species [51]. As this receptor does not have any native co-crystallized ligand, the natural compounds were compared to Tobramycin and 3-oxo-C12-HSL as positive controls. Figure 3c shows the docking score differentiation between the selected structures and positive controls. All three compounds showed a significant increase in the docking score in comparison with the positive controls.

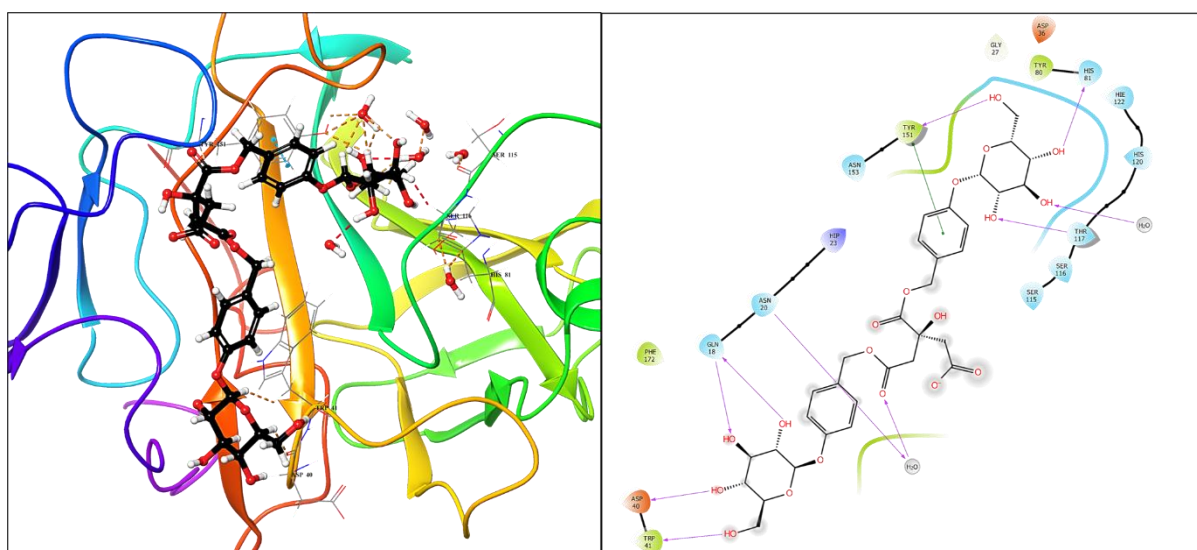


**Figure 6.** The 2D and 3D interaction of the LasA - Parishin complex. The 2D map shows the importance of the involved amino acid in the active site.

### 3.1.4. LasR-TP4.

No preceding reported activity for NP-301, NP-302 were found in the literature. Among positive controls, both Tobramycin and the native co-crystallized ligand of the receptor, 4-Bromo-2-((2-chlorobenzamido) methyl)-6-methylphenyl-2,4-dichlorobenzene, displayed a high docking score and affinity for LasR-TP4. However, the selected structures showed more affinity for the mentioned receptor (Figure 3d). Compound NP-301 with a docking score of -13.175 kcal/mol and free binding energy of -87.824 kcal/mol became the best LasR-TP4 inhibitor. In this compound, the benzene ring forms a stacking bond with amino acid Tyr47, a salt bridge bond between amino groups and Asp73. In addition, a hydrogen bond was

established between the hydroxyl group of the tetrahydrofuran ring and Thr75. Secondary amine interacts with Asp73 (Figure 7).

### 3.1.5. ATPase Type IV pilus.

Similar to the LasR-TP4, there is no record of the biological activity of NP-401 to NP-403. Within the positive controls of this enzyme, the enzyme's native ligand (Phosphomethyl phosphonic acid adenylate ester) has the highest affinity for ATPase Type IV pilus with the docking score of -7.988 kcal/mol. On the other hand, structures NP-401, NP-402, and NP-403 showed the best *in-silico* inhibition activities (-16.274, -15.773, and -15.405 kcal/mol, respectively) for the ATPase Type IV pilus in comparison with the positive controls as well as the other promising candidates for the other four targets (Figure 3e). In compound NP-401, the carboxylate group establishes a hydrogen bond with Gly135, Lys136, Ser137. Other amino acids involved include Thr98, Thr139, and Glu204 (Figure 8).

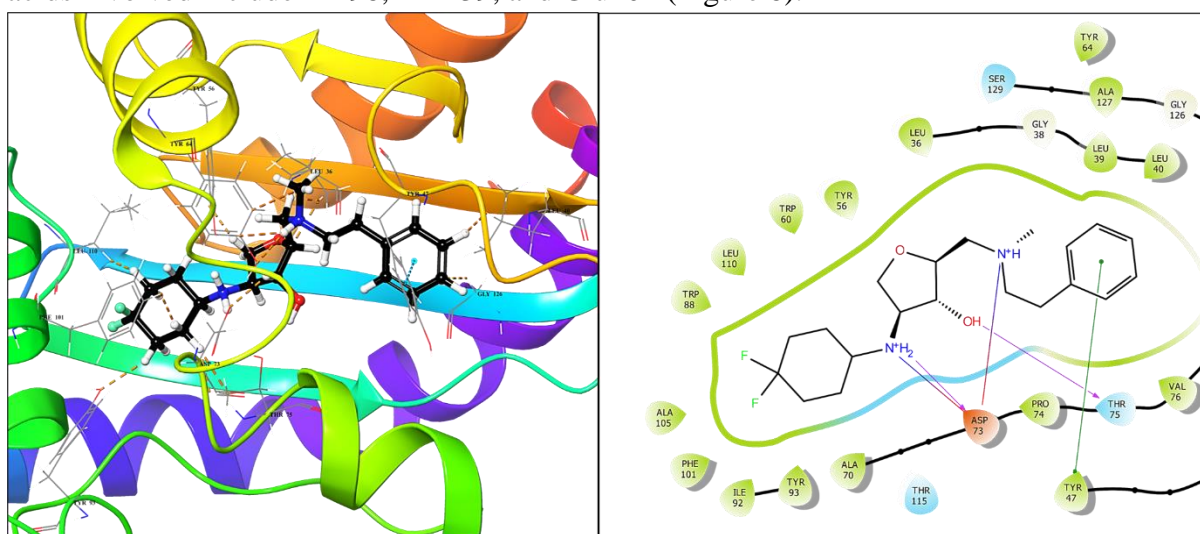


**Figure 7.** The 2D and 3D interaction of the LasR-TP4 - ZINC000514288841 complex. The 2D map shows the importance of the involved amino acid in the active site.

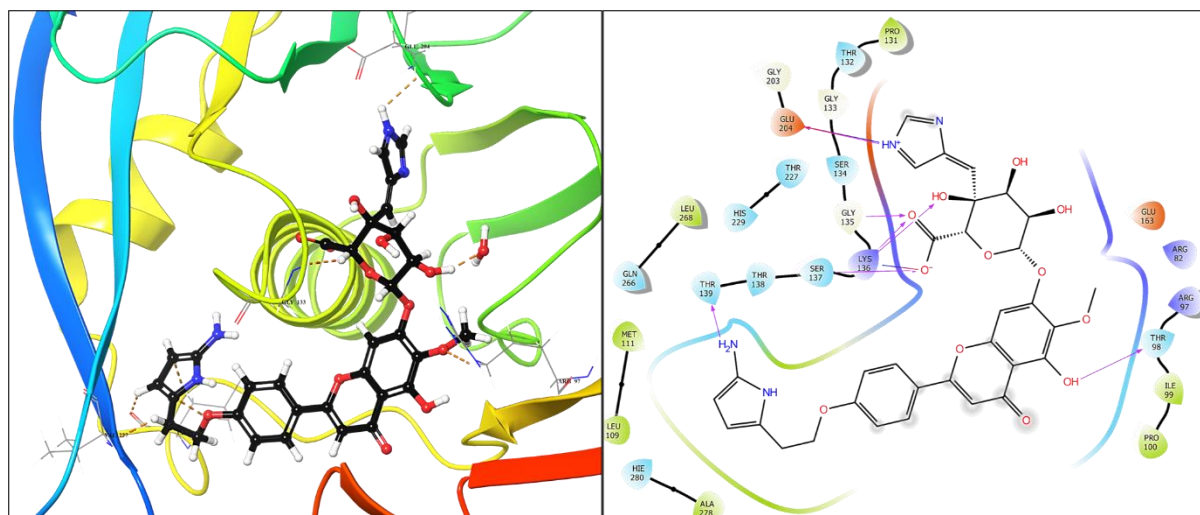


**Figure 8.** The 2D and 3D interaction of the ATPase Type IV pilus - ZINC000150351649 complex. The 2D map shows the importance of the involved amino acid in the active site.

### 3.2. Pharmacokinetic characteristics.

Bioavailability properties for the 15 final compounds are summarized in Table 3. Compounds with a molecular weight of 130 to 725 g/mol, hydrogen bond donors of 0 to 6,

hydrogen bond acceptors of 2 to 20, octanol/water partition coefficient of -2 to 6.5, CNS of -2 (inactive) to +2 (active) and PSA of 7 to 200 Å are in the acceptable range. 3,6'-di-O-sinapoylsucrose (NP-1) with a molecular weight of 586.54 g/mol and CNS of -2 was not able to cross the blood-brain barrier and was therefore considered inactive. Compounds of NP-103, NP-102, and NP-101 showed 100, 76.89, and 65.91% oral absorption, respectively. All listed properties for these compounds except CNS for NP-103 were acceptable. NP-201 showed a CNS of -2, logP of -1.878, and molecular weight of 728.65 g/mol. Compounds NP-103, NP-301, and NP-302 displayed 100, 86.95, and 73.69% oral absorption, respectively. The NP-301 and NP-103 with CNS of +2 are active and can cross the blood-brain barrier. The rest of the predicted characteristics for these three compounds were appropriate. Finally, compounds NP-401, NP-402, and NP-403 do not cross the blood-brain barrier, but their oral absorption is zero.

**Table 3.** Pharmacokinetic properties of natural compounds.

No.	Compound	PSA	MW	H-Do	H-Ac	Log P	Abs. (%)	CNS
NP-1	3,6'-di-O-sinapoylsucrose	283.3	586.54	10	25.6	-4.310	0	-2
NP-2	ZINC000257412737	269.4	504.44	11	27.2	-5.382	0	-2
NP-3	3-O-β-D-rutinosin	244.7	594.52	8	19.8	-1.602	0	-2
NP-101	ZINC000077264779	112.8	392.46	4	10.15	0.999	65.91	-2
NP-102	ZINC000225518732	79.9	388.45	2	9.6	1.268	76.89	1
NP-103	ZINC000096269362	45.1	383.87	1	5.45	4.052	100	2
NP-201	Parishin	325.4	728.65	9	24.25	-1.878	0	-2
NP-202	7-O-galloyl-D-sedoheptulose	222.7	362.29	7	13.75	-2.777	0	-2
NP-203	1,2-di-O-galloyl-6-O-p-coumaroyl-β-D-glucose	297.7	630.51	9	16.35	-0.936	0	-2
NP-301	ZINC000514288841	45.9	368.47	2	6.9	2.886	86.95	2
NP-302	ZINC000077264754	89.5	390.50	3	9.4	1.771	73.69	-2
NP-103	ZINC000096269362	44.4	383.87	1	5.45	3.96	100	2
NP-401	ZINC000150351649	248.6	662.60	6	14.85	2.149	0	-2
NP-402	ZINC000150351636	275.3	678.61	7	16.55	0.945	0	-2
NP-403	ZINC000150349056	323.2	745.65	9	21.35	-1.183	0	-2

MW = Molecular weight (g/mol); PSA = Polar surface area; H-Ac = No. of hydrogen bond acceptors; H-Do = No. of hydrogen bond donors; CNS = Central nervous system; Abs. (%) = Percentage of human oral absorption; LogP = Predicted octanol/water partition coefficient

## 4. Conclusions

Fast-growing bacterial resistance is a vital concern, hence discovering and developing novel and efficient antibiotics that can defeat bacteria resistance. *P. aeruginosa* is a Gram-negative bacteria responsible for many yearly deaths worldwide. Its advanced quorum-sensing system protects the organism from the human defense system and a broad spectrum of known antibiotics. So, targeting the protective QS system can attenuate the bacterium following its destruction. We used in-silico methods to screen 24,000 natural metabolites against five critical PAO1's QS receptors. After screening entire compounds, the top 100 effective structures for each target were assessed by the extra precision (XP) approach followed by calculating binding energies (MM-GBSA) and ADMET properties. Finally, the best three potent in-silico inhibitors for each of the five QS-involved receptors were identified and reported to be used in further in-vitro and in-vivo studies for antimicrobial activity against *P. aeruginosa*.

## Funding

This research received no external funding.

## Acknowledgments

The authors thank the Research Council of Shahid Beheshti University, Tehran, Iran, for financial support.

## Conflicts of Interest

The authors declare no conflict of interest.

## References

1. Berthelot, P.; Attree, I.; Plésiat, P.; Chabert, J.; de Bentzmann, S.; Pozzetto, B.; Grattard, F. Genotypic and phenotypic analysis of type III secretion system in a cohort of *Pseudomonas aeruginosa* bacteremia isolates: evidence for a possible association between O serotypes and exo genes. *J Infect Dis* **2003**, *188*, 512-518, <https://doi.org/10.1086/377000>.
2. Lyczak, J.B.; Cannon, C.L.; Pier, G.B. Establishment of *Pseudomonas aeruginosa* infection: lessons from a versatile opportunist. *Microb Infect* **2000**, *2*, 1051-1060, [https://doi.org/10.1016/S1286-4579\(00\)01259-4](https://doi.org/10.1016/S1286-4579(00)01259-4).
3. Van Delden, C.; Iglewski, B.H. Cell-to-cell signaling and *Pseudomonas aeruginosa* infections. *Emerg Infect Dis* **1998**, *4*, 551-560.
4. Al-Wrafy, F.; Brzozowska, E.; Górska, S.; Gamian, A. Pathogenic factors of *Pseudomonas aeruginosa*-the role of biofilm in pathogenicity and as a target for phage therapy. *Postepy Hig Med Dosw* **2017**, *71*, 78-91.
5. Miari, M.; Rasheed, S.S.; Ahmad, N.H.; Itani, D.; Abou Fayad, A.; Matar, G.M. Natural products and polysorbates: Potential Inhibitors of biofilm formation in *Pseudomonas aeruginosa*. *J Infect Dev Ctries* **2020**, *14*, 580-588, <https://doi.org/10.3855/jidc.11834>.
6. Saeki, E.K.; Kobayashi, R.K.T.; Nakazato, G. Quorum sensing system: Target to control the spread of bacterial infections. *Microb Pathog* **2020**, *142*, 104068, <https://doi.org/10.1016/j.micpath.2020.104068>.
7. Smith, R.S.; Iglewski, B.H. *Pseudomonas aeruginosa* quorum sensing as a potential antimicrobial target. *J Clin Invest* **2003**, *112*, 1460-1465, <https://doi.org/10.1172/JCI20364>.
8. Soto-Aceves, M.P.; Cocotl-Yañez, M.; Servín-González, L.; Soberón-Chávez, G. The Rhl Quorum-Sensing System Is at the Top of the Regulatory Hierarchy under Phosphate-Limiting Conditions in *Pseudomonas aeruginosa* PAO1. *J Bacteriol* **2021**, *203*, <https://doi.org/10.1128/JB.00475-20>.
9. Mishra, A.; Mishra, N. Antiquorum Sensing Activity of Copper Nanoparticle in *Pseudomonas aeruginosa*: An In Silico Approach. *Proc Natl Acad Sci India B* **2021**, *91*, 29-36, <https://doi.org/10.1007/s40011-020-01193-z>.
10. Gambello, M.J.; Iglewski, B.H. Cloning and characterization of the *Pseudomonas aeruginosa* lasR gene, a transcriptional activator of elastase expression. *J Bacteriol* **1991**, *173*, <https://doi.org/10.1128/jb.173.9.3000-3009.1991>.
11. Pearson, J.P.; Gray, K.M.; Passador, L.; Tucker, K.D.; Eberhard, A.; Iglewski, B.H.; Greenberg, E.P. Structure of the autoinducer required for expression of *Pseudomonas aeruginosa* virulence genes. *Proc Natl Acad Sci* **1994**, *91*, 197-201, <https://doi.org/10.1073/pnas.91.1.197>.
12. Kiratisin, P.; Tucker, K.D.; Passador, L. LasR, a transcriptional activator of *Pseudomonas aeruginosa* virulence genes, functions as a multimer. *J Bacteriol* **2002**, *184*, 4912-4919, <https://doi.org/10.1128/JB.184.17.4912-4919.2002>.
13. Ochsner, U.A.; Koch, A.K.; Fiechter, A.; Reiser, J. Isolation and characterization of a regulatory gene affecting rhamnolipid biosurfactant synthesis in *Pseudomonas aeruginosa*. *J Bacteriol* **1994**, *176*, 2044-2054, <https://doi.org/10.1128/jb.176.7.2044-2054.1994>.
14. Pearson, J.P.; Passador, L.; Iglewski, B.H.; Greenberg, E.P. A second N-acylhomoserine lactone signal produced by *Pseudomonas aeruginosa*. *Proceedings of the National Academy of Sciences* **1995**, *92*, 1490-1494, <https://doi.org/10.1073/pnas.92.5.1490>.
15. Omrani, M.; Bayati, M.; Mehrbod, P.; Bardazard, K.A.; Nejad-Ebrahimi, S. Natural products as inhibitors of COVID-19 main protease—A virtual screening by molecular docking. *Pharmaceutical Sciences* **2021**, *27*, S135-S148, <https://doi.org/10.34172/PS.2021.11>.
16. Fallah, M.S.; Bayati, M.; Najafi, A.; Behmard, E.; Javad, S. Molecular Docking Investigation of Antiviral Herbal Compounds as Potential Inhibitors of SARS-CoV-2 Spike Receptor. *Biointerface Research in Applied Chemistry* **2021**, *11*, 12916-12924, <https://doi.org/10.33263/BRIAC115.1291612924>.
17. Khan, M.S.; Qais, F.A.; Ahmad, I. Quorum sensing interference by natural products from medicinal plants: Significance in combating bacterial infection. In *Biotechnological applications of quorum sensing inhibitors* **2018**, 417-445, [https://doi.org/10.1007/978-981-10-9026-4\\_20](https://doi.org/10.1007/978-981-10-9026-4_20).
18. Malka, O.; Kalson, D.; Yaniv, K.; Shafir, R.; Rajendran, M.; Ben-David, O.; Kushmaro, A.; Meijler, M.M.; Jelinek, R. Cross-kingdom inhibition of bacterial virulence and communication by probiotic yeast metabolites. *Microbiome* **2021**, *9*, <https://doi.org/10.1186/s40168-021-01027-8>.



19. Ganesh, P.S.; Rai, V.R. Attenuation of quorum-sensing-dependent virulence factors and biofilm formation by medicinal plants against antibiotic resistant *Pseudomonas aeruginosa*. *J Tradit Complement Med* **2018**, *8*, 170-177, <https://doi.org/10.1016/j.jtcme.2017.05.008>.
20. Maisuria, V.B.; Lopez-de Los Santos, Y.; Tufenkji, N.; Déziel, E. Cranberry-derived proanthocyanidins impair virulence and inhibit quorum sensing of *Pseudomonas aeruginosa*. *Scientific reports* **2016**, *6*, <https://doi.org/10.1038/srep30169>.
21. Pérez-López, M.; Flores-Cruz, M.; Martínez-Vázquez, M.; Soto-Hernández, M.; García-Contreras, R.; Padilla-Chacón, D.; Castillo-Juárez, I. Anti-virulence activities of some Tillandsia species (Bromeliaceae). *Bot Sci* **2020**, *98*, 117-127, <https://doi.org/10.17129/botsci.2380>.
22. Chu, W.; Zhou, S.; Jiang, Y.; Zhu, W.; Zhuang, X.; Fu, J. Effect of traditional Chinese herbal medicine with anti-quorum sensing activity on *Pseudomonas aeruginosa*. *Evid Based Complement Alternat Med* **2013**, *2013*, <https://doi.org/10.1155/2013/648257>.
23. Kong, J.; Wang, Y.; Xia, K.; Zang, N.; Zhang, H.; Liang, X. New insights into the antibacterial and quorum sensing inhibition mechanism of Artemisia argyi leaf extracts towards *Pseudomonas aeruginosa* PAO1. *3 Biotech* **2021**, *11*, <https://doi.org/10.1007/s13205-021-02663-5>.
24. Gould, T.A.; Schweizer, H.P.; Churchill, M.E. structure of the *Pseudomonas aeruginosa* acyl-homoserinelactone synthase LasI. *Mol Microbiol* **2004**, *53*, 1135-1146, <https://doi.org/10.1111/j.1365-2958.2004.04211.x>.
25. Bottomley, M.J.; Muraglia, E.; Bazzo, R.; Carfi, A. Molecular insights into quorum sensing in the human pathogen *Pseudomonas aeruginosa* from the structure of the virulence regulator LasR bound to its autoinducer. *J Biol Chem* **2007**, *282*, 13592-13600, <https://doi.org/10.1074/jbc.M700556200>.
26. Spencer, J.; Murphy, L.M.; Connors, R.; Sessions, R.B.; Gamblin, S.J. Crystal structure of the LasA virulence factor from *Pseudomonas aeruginosa*: substrate specificity and mechanism of M23 metalloproteases. *J Mol Biol* **2010**, *396*, 908-923, <https://doi.org/10.1016/j.jmb.2009.12.021>.
27. Zou, Y.; Nair, S.K. Molecular basis for the recognition of structurally distinct autoinducer mimics by the *Pseudomonas aeruginosa* LasR quorum-sensing signaling receptor. *Chem Biol* **2009**, *16*, 961-970, <https://doi.org/10.1016/j.chembiol.2009.09.001>.
28. Misić, A.M.; Satyshur, K.A.; Forest, K.T. *P. aeruginosa* PilT structures with and without nucleotide reveal a dynamic type IV pilus retraction motor. *J Mol Biol* **2010**, *400*, 1011-1021, <https://doi.org/10.1016/j.jmb.2010.05.066>.
29. Bhardwaj, S.; Bhatia, S.; Singh, S.; Franco Jr, F. Growing emergence of drug-resistant *Pseudomonas aeruginosa* and attenuation of its virulence using quorum sensing inhibitors: A critical review. *Iran J Basic Med Sci* **2021**, *24*, 699-719, <https://dx.doi.org/10.22038/2FIJBMS.2021.49151.11254>.
30. Elmanama, A.A.; Al-Reefi, M.R. Antimicrobial, anti-biofilm, anti-quorum sensing, antifungal and synergistic effects of some medicinal plants extracts. *IUG j nat eng stud* **2017**.
31. Zhang, A.; Chu, W.-H. Anti-quorum sensing activity of Forsythia suspense on Chromobacterium violaceum and *Pseudomonas aeruginosa*. *Pharmacogn Mag* **2017**, *13*, 321-325, <https://dx.doi.org/10.4103/2F0973-1296.204547>.
32. Rahman, M.R.T.; Lou, Z.; Yu, F.; Wang, P.; Wang, H. Anti-quorum sensing and anti-biofilm activity of Amomum tsaoko (Amomum tsao-ko Crevost et Lemarie) on foodborne pathogens. *Saudi J Biol Sci* **2017**, *24*, 324-330, <https://doi.org/10.1016/j.sjbs.2015.09.034>.
33. Rekha, P.; Vasavi, H.; Vipin, C.; Saptami, K.; Arun, A. A medicinal herb Cassia alata attenuates quorum sensing in Chromobacterium violaceum and *Pseudomonas aeruginosa*. *Lett Appl Microbiol* **2017**, *64*, 231-238, <https://doi.org/10.1111/lam.12710>.
34. Husain, F.M.; Ahmad, I.; Khan, M.S.; Ahmad, E.; Tahseen, Q.; Khan, M.S.; Alshabib, N.A. Sub-MICs of Mentha piperita essential oil and menthol inhibits AHL mediated quorum sensing and biofilm of Gram-negative bacteria. *Front microbiol* **2015**, *6*, 420, <https://doi.org/10.3389/fmicb.2015.00420>.
35. Husain, F.M.; Ahmad, I.; Khan, M.S.; Al-Shabib, N.A. Trigonella foenum-graceum (Seed) extract interferes with quorum sensing regulated traits and biofilm formation in the strains of *Pseudomonas aeruginosa* and Aeromonas hydrophila. *Evid Based Complement Alternat Med* **2015**, *2015*, <https://doi.org/10.1155/2015/879540>.
36. Ghosh, R.; Tiwary, B.K.; Kumar, A.; Chakraborty, R. Guava leaf extract inhibits quorum-sensing and Chromobacterium violaceum induced lysis of human hepatoma cells: whole transcriptome analysis reveals differential gene expression. *PLoS One* **2014**, *9*, e107703, <https://doi.org/10.1371/journal.pone.0107703>.
37. Rasamiravaka, T.; Jedrzejowski, A.; Kiendrebeogo, M.; Rajaonson, S.; Randriamampionona, D.; Rabemanantsoa, C.; Andriantsimahavandy, A.; Rasamindrakotroka, A.; Duez, P.; El Jaziri, M. Endemic Malagasy Dalbergia species inhibit quorum sensing in *Pseudomonas aeruginosa* PAO1. *Microbiology* **2013**, *159*, 924-938, <https://doi.org/10.1099/mic.0.064378-0>.
38. Bayati, M.; Ebrahimi, S.N. Blocking Effect of Natural Alkaloids on COVID-19 Pentameric Ion Channel: An in silico Perspective. *Biointerface Research in Applied Chemistry* **2022**, *12*, 4961-4973, <http://dx.doi.org/10.33263/BRIAC124.49614973>.



39. De Leo, M.; Peruzzi, L.; Granchi, C.; Tuccinardi, T.; Minutolo, F.; De Tommasi, N.; Braca, A. Constituents of *Polygala flavescens* ssp. *flavescens* and their activity as inhibitors of human lactate dehydrogenase. *J Nat Prod* **2017**, *80*, 2077-2087, <https://doi.org/10.1021/acs.jnatprod.7b00295>.
40. Zhou, D.; Wei, H.; Jiang, Z.; Li, X.; Jiao, K.; Jia, X.; Hou, Y.; Li, N. Natural potential neuroinflammatory inhibitors from *Alhagi sparsifolia* Shap. *Bioorganic Med Chem Lett* **2017**, *27*, 973-978, <https://doi.org/10.1016/j.bmcl.2016.12.075>.
41. Lin, J.-H.; Liu, Y.-C.; Hau, J.-P.; Wen, K.-C. Parishins B and C from rhizomes of *Gastrodia elata*. *Phytochemistry* **1996**, *42*, 549-551, [https://doi.org/10.1016/0031-9422\(95\)00955-8](https://doi.org/10.1016/0031-9422(95)00955-8).
42. Lee, C.M.; Jung, H.A.; Oh, S.H.; Park, C.H.; Tanaka, T.; Yokozawa, T.; Choi, J.S. Kinetic and molecular docking studies of loganin and 7-O-galloyl-D-sedoheptulose from *Corni Fructus* as therapeutic agents for diabetic complications through inhibition of aldose reductase. *Arch Pharm Res* **2015**, *38*, 1090-1098, <https://doi.org/10.1007/s12272-014-0493-3>.
43. Yamabe, N.; Kang, K.S.; Matsuo, Y.; Tanaka, T.; Yokozawa, T. Identification of antidiabetic effect of iridoid glycosides and low molecular weight polyphenol fractions of *Corni Fructus*, a constituent of *Hachimi-jio-gan*, in streptozotocin-induced diabetic rats. *Biol Pharm Bull* **2007**, *30*, 1289-1296, <https://doi.org/10.1248/bpb.30.1289>.
44. Yamabe, N.; Kang, K.S.; Park, C.H.; Tanaka, T.; Yokozawa, T. 7-O-galloyl-D-sedoheptulose is a novel therapeutic agent against oxidative stress and advanced glycation endproducts in the diabetic kidney. *Biol Pharm Bull* **2009**, *32*, 657-664, <https://doi.org/10.1248/bpb.32.657>.
45. Yamabe, N.; Noh, J.S.; Park, C.H.; Kang, K.S.; Shibahara, N.; Tanaka, T.; Yokozawa, T. Evaluation of loganin, iridoid glycoside from *Corni Fructus*, on hepatic and renal glucolipotoxicity and inflammation in type 2 diabetic db/db mice. *Eur J Pharmacol* **2010**, *648*, 179-187, <https://doi.org/10.1016/j.ejphar.2010.08.044>.
46. Park, C.H.; Tanaka, T.; Yokozawa, T. Anti-diabetic action of 7-O-galloyl-D-sedoheptulose, a polyphenol from *Corni Fructus*, through ameliorating inflammation and inflammation-related oxidative stress in the pancreas of type 2 diabetics. *Biol Pharm Bull* **2013**, *36*, 723-732, <https://doi.org/10.1248/bpb.b12-00543>.
47. Park, C.H.; Noh, J.S.; Kim, J.H.; Tanaka, T.; Zhao, Q.; Matsumoto, K.; Shibahara, N.; Yokozawa, T. Evaluation of morroniside, iridoid glycoside from *Corni Fructus*, on diabetes-induced alterations such as oxidative stress, inflammation, and apoptosis in the liver of type 2 diabetic db/db mice. *Biol Pharm Bull* **2011**, *34*, 1559-1565, <https://doi.org/10.1248/bpb.34.1559>.
48. Yokozawa, T.; Kang, K.S.; Park, C.H.; Noh, J.S.; Yamabe, N.; Shibahara, N.; Tanaka, T. Bioactive constituents of *Corni Fructus*: The therapeutic use of morroniside, loganin, and 7-O-galloyl-D-sedoheptulose as renoprotective agents in type 2 diabetes. *Drug Discov Ther* **2010**, *4*, 223-234.
49. Gao, X.; Liu, Y.; An, Z.; Ni, J. Active Components and Pharmacological Effects of *Cornus officinalis*: Literature Review. *Front Pharmacol* **2021**, *12*, 513, <https://doi.org/10.3389/fphar.2021.633447>.
50. Ma, D.; Li, Y.; Zhu, Y.; Wei, W.; Zhang, L.; Li, Y.; Li, L.; Zhang, L. Cornel iridoid glycoside ameliorated Alzheimer's disease-like pathologies and necroptosis through RIPK1/MLKL pathway in young and aged SAMP8 mice. *Evid Based Complement Alternat Med* **2021**, *2021*, <https://doi.org/10.1155/2021/9920962>.
51. Kashiwada, Y.; Nonaka, G.-I.; Nishioka, I.; Yamagishi, T. Galloyl and hydroxycinnamoylglucoses from rhubarb. *Phytochemistry* **1988**, *27*, 1473-1477, [https://doi.org/10.1016/0031-9422\(88\)80218-8](https://doi.org/10.1016/0031-9422(88)80218-8).